Confinement Effect of Concrete with Carbon Fiber Sheet Reinforcement under Compressive Loading

Roy Reyna, Taiki Saito, Tomoya Matsui, and Kazuhiro Hayashi
Department of Architecture and Civil Engineering, Toyohashi University of Technology, Toyohashi, Japan
Email: royanyer@gmail.com, {tsaito, matsui, hayashi}@ace.tut.ac.jp

***Abstract*—Over the past 15 years, large scale construction of medium-rise buildings, built using Low Ductility Reinforced Concrete (LDRC) wall, have been commonplace in Peru. These walls do not have boundary columns and have a small quantity of reinforcing bars at each end, therefore is expected to fail in flexural mode. From past studies, where a retrofitting method was proposed by using Carbon fibEr Sheet (CFS) over the LDRC wall, it was verified that CFS delays the concrete crushing of the wall base that occurs during flexural failure and that deformation capacity was improved. In order to verify the confinement effect of the carbon fiber sheet over the concrete, an experiment was conducted using concrete samples with CFS by changing the size, shape and amount of CFS layers. In total, 39 concrete samples were tested under compressive loading (monotonic and cyclic). From the experiment, it was confirmed that deformation performance improved and the strength of the concrete was increased due to the confinement. However, it should be noted that the stress-strain relationship of concrete with CFS depends on the shape of the concrete sample.**

***Index Terms*—reinforced concrete, carbon fiber sheet, confinement effect**

I. Introduction

Over the last 15 years, large scale construction of medium-rise buildings have been commonplace in Peru that use low ductility reinforced concrete walls, with rectangular cross-sections, reinforced with wire mesh and additional vertical reinforcing bars at boundary ends [1]. These walls do not have boundary columns and have only a small quantity of reinforcing bars at each end, therefore is expected to fail in flexural mode.

Two experiments were conducted on Low Ductility Reinforced Concrete (LDRC) wall with and without Carbon Fiber Sheet (CFS) as a retrofitting method. The first experiment was conducted in 2013 at the Toyohashi University of Technology (TUT) on three LDRC walls [2], the first wall was without CFS reinforcement, the second wall was wrapped completely with CFS and the third wall was wrapped with CFS at the edges only. The second experiment was conducted in 2014 at TUT on three LDRC walls, following the same retrofitted pattern of the first experiment but with partial retrofitting with CFS to a specified height.

From those tests, it was verified that the carbon fiber sheets delay the concrete crushing of the wall base that occurs during the flexural failure and that deformation capacity was improved. Moreover, during the test with the retrofitted walls it was observed that the crushing of the concrete produces bulges at the base corners of the wall. Additionally, when the maximum strain on the CFS is reached, the carbon fiber sheet over the crushed concrete area fails suddenly.

In order to verify the confinement effect of the carbon fiber sheet that covers the concrete, a third experiment was conducted in 2015 at TUT using concrete samples with and without CFS, by changing the size, shape and amount of CFS layers. Characteristics of the specimens were decided following Lam and Teng's research [3]-[5] and Nakatsuka's research [6], further studies will focus on the stress-strain relationship of the CFS confined concrete.

II. Outline of the Test

A. Specimens

In total, 39 concrete samples were tested under compressive loading (monotonic and cyclic). The specimens have three kinds of cross section shapes: circular (C), square (S) and rectangular (R); the ratio of each specimen corresponds to the ratio of $(w/b)(h/b)$, where b, w and h are the thickness, width and height of the specimen respectively. Table I shows the dimensions and quantities of each specimen.

29 specimens were retrofitted using carbon fiber sheet wrapped over the lateral surface of the specimen by using chemical epoxy. Table II shows the materials properties of the different carbon fiber sheet used to retrofit the concrete samples. Where ρ_f, is the density per unit of area of CFS, t, is the thickness of CFS, E_f, is the young modulus of CFS, σ_{fu}, is the ultimate tensile strength of CFS and ε_{fu}, is the ultimate tensile strain of CFS.

All square and rectangular specimens has a chamfer radius R = 15mm, except for 4 specimens with R = 30mm. Besides, one circular and one square shaped specimen where retrofitted using a CFS with higher young modulus

Manuscript received December 4, 2015; revised May 4, 2016.

doi: 10.18178/ijscer.5.4.250-257

(CFS-3). Finally, 2 specimens where retrofitted by fixing the CFS with steel plates and bolts.

Each specimen was allocated a code which represents the geometry of the specimen, type of CFS and special conditions. (See Table III).

TABLE I. TYPE OF SPECIMENS

Shape	Ratio	b (mm)	w (mm)	h (mm)	Quantity
C	2	ϕ 150		300	8
S	12	150	150	300	9
S	13	150	150	450	2
R	22	150	300	300	4
R	23	150	300	450	2
R	32	100	300	200	5
R	33	100	300	300	2
R	42	100	400	200	5
R	43	100	400	300	2

TABLE II. MATERIAL PROPERTIES OF CARBON FIBER SHEET

CFS	ρ_f (g/m^2)	t (mm)	E_f (MPa)	σ_{fu} (MPa)	ε_{fu} (%)
1	200	0.111	249000	4283	1.72
2	300	0.167	249000	4681	1.88
3	300	0.163	444000	3241	0.73

TABLE III. SPECIMEN CODE

XY-WZ :	Specimen code	
X :	Specimen shape (See Table II)	
Y :	Specimen ratio (See Table II)	
W :	Type of CFS (See Table I)	
	0 :	Concrete only
	2 :	1 Layer, CFS-1 (200g/m^2)
	3 :	1 Layers, CFS-2 (300g/m^2)
	4 :	2 Layer, CFS-1 (200g/m^2)
	6 :	2 Layers, CFS-2 (300g/m^2)
Z :	Special considerations (*)	
	C :	Static reversal loading
	R :	R=30mm (**)
	E :	CFS-3 is used instead of CFS-2
	B :	Fixed with bolts

(*) No character means monotonic test.

(**) R is the chamfer radius of the specimen. For other cases R=15mm

B. Loading Program

Two types of test were conducted:

- Monotonic test, where the specimen is under compressive load until failure.
- Static reversal loading, where the specimen is under a cyclic load until failure. (See Fig. 1)

Fig. 2 shows the compression loading machine used for the experiment with a maximum compression loading of 2000kN. Table IV shows the type of loading for each specimen and condition

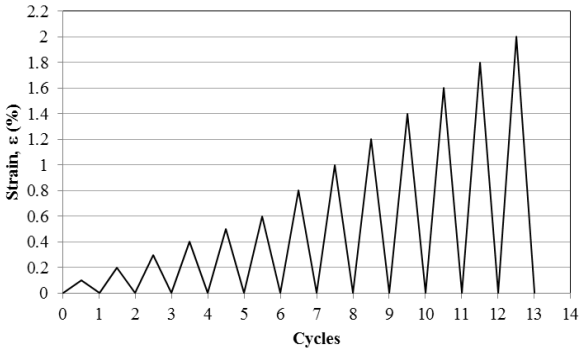

Figure 1. Loading pattern for cyclic test.

Figure 2. Compression loading machine.

TABLE IV. LOADING TEST

XY	WZ									
	0	0C	2	3	3C	3R	3E	3B	4	6
C2	○	○	○	○	○		○		○	○
S12	○	○	○	○	○	○	○		○	○
S13	○			○						
R22	○		○	○		○				
R23	○			○						
R32	○		○	○		○		○		
R33	○			○						
R42	○		○	○		○		○		
R43	○			○						

C. Measuring Method

The vertical displacement of the concrete along the compressive direction was measured using displacement transducers for all the specimens, as is shown in Fig. 3. In the case of the retrofitted specimens with CFS, the horizontal strain of the CFS was measured using strain gauges. Specimens with CFS and strain gages are shown in Fig. 4.

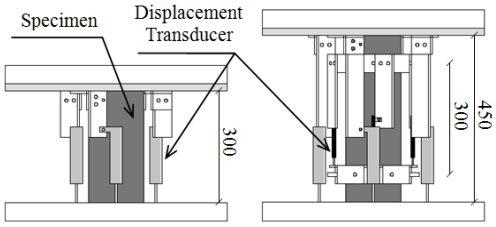

Figure 3. Arrangement of measuring devices (unit: mm).

Figure 4. Arrangement of measuring devices (unit: mm).

III. Test Result

A. Circular Shape

Fig. 5 corresponds to the specimens C2 under monotonic loading. The maximum strength of the concrete, f'_c, without CFS (C2-0) is 36.03MPa, the strain corresponding to the maximum strength, ε_{cu}, is 0.0024. Table V shows the maximum strength and maximum strain for each specimen C2 under monotonic and cyclic loading.

TABLE V. Maximum Strength and Strain of Circular Shape

Specimen	Maximum Strength (MPa)	Strain (%) at Maximum Strength	Maximum Strain (%)
C2-0	36.03	0.24	1.54
C2-0C	35.56	0.23	1.19
C2-2	42.96	1.01	1.01
C2-3	53.73	1.44	1.44
C2-3C	55.70	1.94	1.94
C2-3E	43.87	0.50	0.50
C2-4	74.11	2.38	2.38
C2-6	88.12	2.87	2.87

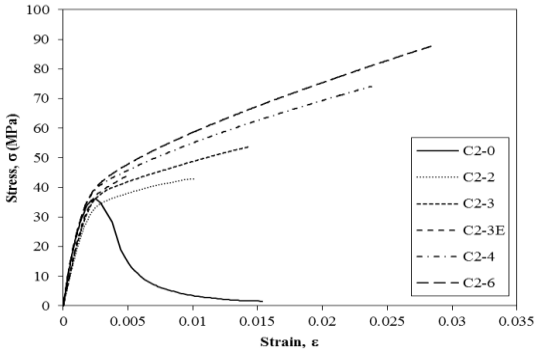

Figure 5. Stress-strain of concrete – Specimens C2 under monotonic loading.

Fig. 6 corresponds to the specimens C2 under cyclic loading, specimen C2-0C (concrete only) and specimen C2-3C with CFS. The contribution of the CFS confinement by increasing the maximum strength and the maximum strain can be observed.

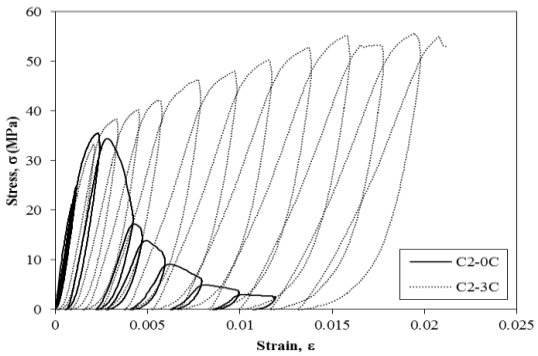

Figure 6. Stress-strain of concrete – Specimens C2 under cyclic loading.

Fig. 7 shows specimens C2-0 and C2-0C (concrete only) corresponding to the monotonic curve and cyclic curve respectively; the monotonic curve follows the shape of the envelope of the cyclic curve. In the same way, Fig. 8 shows the good match between specimens C2-3 and C2-3C corresponding to the monotonic curve and cyclic curve respectively.

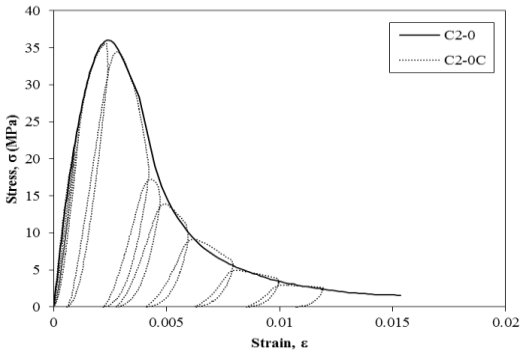

Figure 7. Stress-strain of concrete – Comparison between the monotonic and cyclic loading of specimen C2 without CFS.

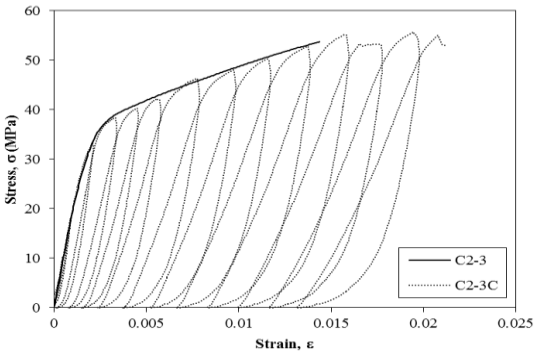

Figure 8. Stress-strain of concrete – Comparison between the monotonic and cyclic loading of specimen C2 with CFS.

During the failure mode with the circular shaped specimens (C2) retrofitted with CFS a sudden failure occurs when maximum strength is reached. This can be explained as the deformation of the concrete applies about the same level of stress on the CFS. Fig. 9 shows

the failure sequence: (a) shows the state of the specimen before reaching the maximum strength, (b) shows the state of the specimen when the maximum strength is reached; after this, the strength drops suddenly (c) shows the remaining core of concrete and (d) shows the state of the specimen after the crushing of concrete.

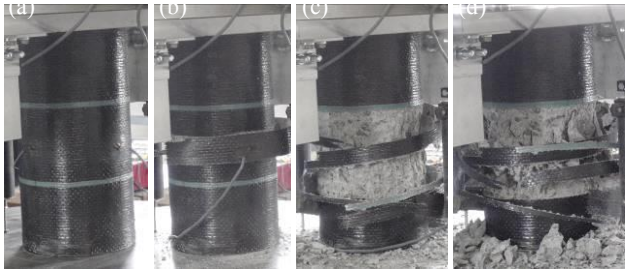

Figure 9. Failure mode of specimen C2 with CFS.

B. Square Shape

Fig. 10 and Fig. 11 correspond to the specimens S12 and S13 respectively, under monotonic loading. Both, Fig. 10 and Fig. 11 show a discrepancy in terms of the maximum strength of the concrete between the non-retrofitted sample and the sample retrofitted with CFS; where specimens with CFS have a higher maximum strength than the non-retrofitted specimen. Table VI shows the maximum strength and maximum strain for each specimen, S12 and S13, under monotonic and cyclic loading.

Fig. 12 corresponds to the specimens S12 under cyclic loading, specimen S12-0C (concrete only) and specimen S12-3C with CFS. The contribution of the CFS confinement can be observed by increasing the maximum strain, but not the maximum strength, which remains about the same.

Fig. 13 shows a slight discrepancy in terms of the maximum strength between the monotonic curve (S12-0) and the cyclic curve (S12-0C), where specimen S12-0 has a lower strength than specimen S12-0C.

On the other hand, Fig. 14 shows the comparison between the monotonic curve (Specimen S12-3) and the cyclic curve (Specimen S12-3C), where specimen S12-3 has a greater strength than specimen S12-3C.

TABLE VI. MAXIMUM STRENGTH AND STRAIN OF SQUARE SHAPE

Specimen	Maximum Strength (MPa)	Strain (%) at Maximum Strength	Maximum Strain (%)
S12-0	33.34	0.26	1.58
S12-0C	38.46	0.27	1.16
S12-2	42.21	0.38	1.06
S12-3	43.83	0.38	1.35
S12-3C	39.55	0.42	2.55
S12-3R	43.93	0.50	1.44
S12-3E	43.62	0.43	0.73
S12-4	41.89	0.50	1.79
S12-6	45.55	0.42	2.45
S13-0	38.20	0.24	0.50
S13-3	41.46	0.30	1.44

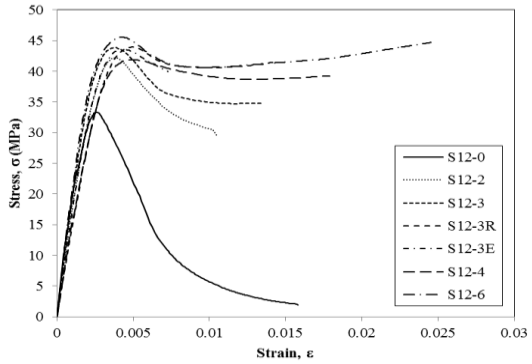

Figure 10. Stress-strain of concrete – Specimen S12 under monotonic loading.

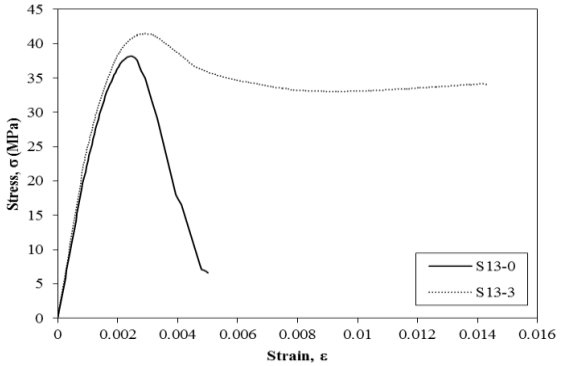

Figure 11. Stress-strain of concrete – Specimen S13 under monotonic loading.

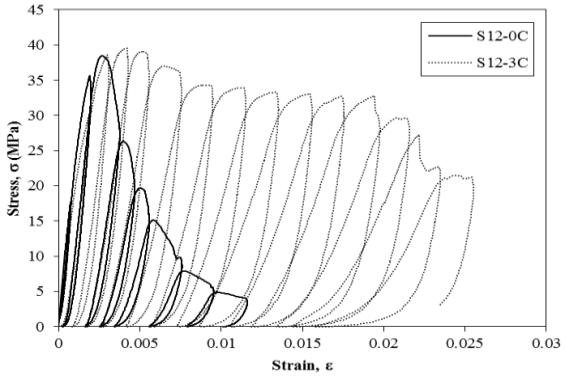

Figure 12. Stress-strain of concrete – Specimen S12 under cyclic loading.

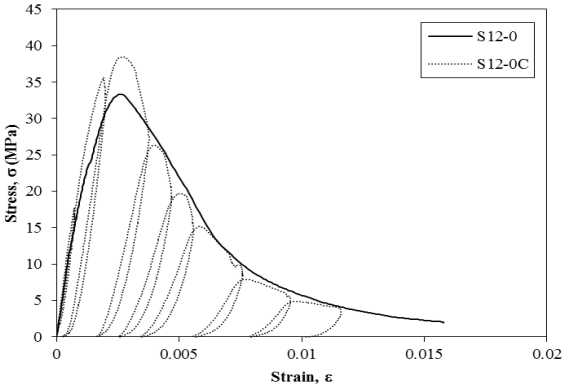

Figure 13. Stress-strain of concrete – Comparison between the monotonic and cyclic loading of specimen S12 without CFS.

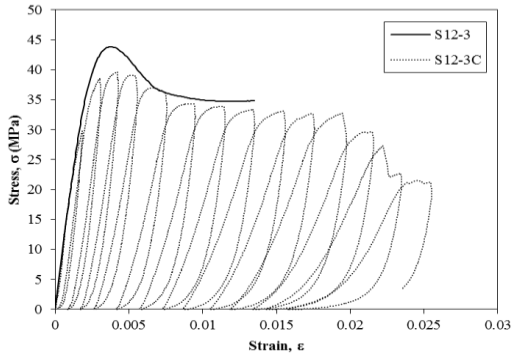

Figure 14. Stress-strain of concrete – Comparison between the monotonic and cyclic loading of specimen S12 with CFS.

In the failure mode with the square shaped specimens (S12 and S13) retrofitted with CFS, a two-step failure occurs; due to the stress on the CFS concentrated at the rounded corners of the specimen. Fig. 15 shows the failure sequence: (a) shows the state of the specimen before reaching the maximum strength, (b) shows the state of the specimen after the maximum strength is reached, the strength decreases and the strain deformation capacity is improved, (c) shows the state of the specimen when CFS fails first at one corner releasing partially the confinement provided by CFS and (d) shows the state of the specimen when the CFS fails at the opposite corner. This study will consider the stress-strain relationship until the first CFS failure.

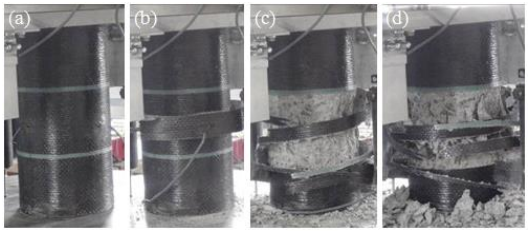

Figure 15. Failure mode of specimen S12 with CFS.

C. Rectangular Shape

Fig. 16, Fig. 17, Fig. 18, Fig. 19, Fig. 20 and Fig. 21 corresponds to the specimens R22, R23, R32, R33, R42 and R43 respectively under monotonic loading. The maximum strength and strain for each specimen is shown in Table VII.

TABLE VII. MAXIMUM STRENGTH AND STRAIN OF RECTANGULAR SHAPE

Specimen	Maximum Strength (MPa)	Strain (%) at Maximum Strength	Maximum Strain (%)
R22-0	37.74	0.33	0.45
R22-2	36.61	0.38	0.72
R22.3	36.85	0.42	0.63
R22-3R	37.87	0.42	1.68
R23-0	30.02	0.23	0.33
R23-3	36.71	0.40	1.09
R32-0	42.34	0.32	0.41
R32-2	39.80	0.34	4.83
R32-3	39.01	0.54	2.34
R32-3R	49.93	0.68	3.22
R32-B	40.90	0.38	2.32
R33-0	39.10	0.27	0.34
R33-3	39.87	0.32	0.32
R42-0	43.47	0.33	0.39
R42-2	40.05	0.38	1.94
R42-3	38.59	0.51	0.58
R42-3R	46.01	0.58	2.55
R42-3B	40.68	0.37	2.64
R43-0	35.89	0.27	0.34
R43-3	32.60	0.39	1.87

Specimens R22 and R33, in Fig. 16 and 19 respectively, shows a relatively close maximum strength in all of the specimens. However, Fig. 17, 18, 20 and 21, corresponding to specimens R23, R32, R42 and R43, show a discrepancy in terms of the maximum strength.

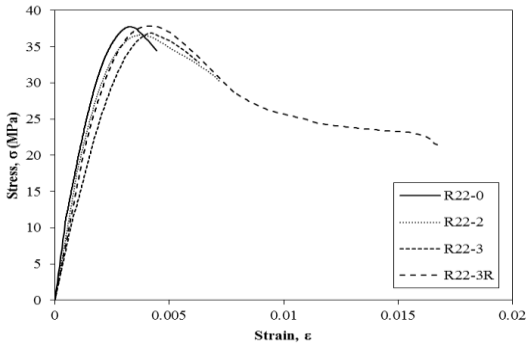

Figure 16. Stress-strain of concrete – Specimens R22 under monotonic loading.

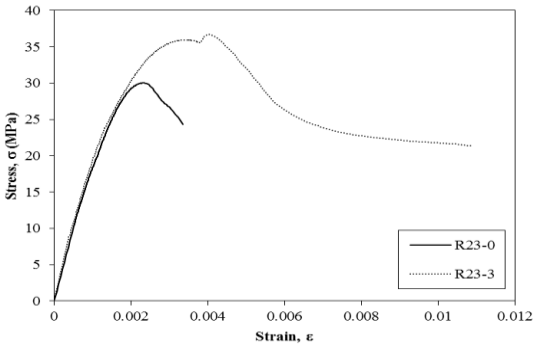

Figure 17. Stress-strain of concrete – Specimens R23 under monotonic loading.

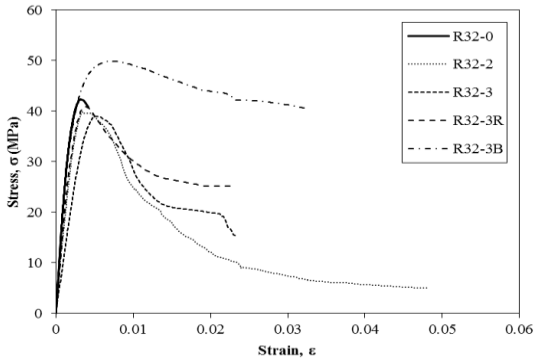

Figure 18. Stress-strain of concrete – Specimens R32 under monotonic loading.

The failure mode of rectangular shaped specimens (R22, R23, R32, R33, R42 and R43) retrofitted with CFS fails in a similar way to the square shaped specimens.

IV. Analysis of the Result

From the test result, the effect of the parameters such as the shape effect, the amount of CFS, the chamfer radius, the Young Modulus of the CFS and the usage of bolts for fixing the CFS is studied in this research.

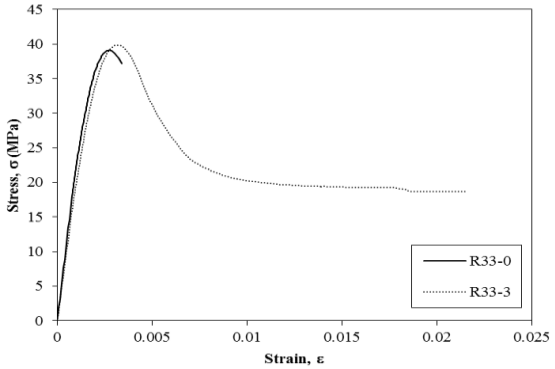

Figure 19. Stress-strain of concrete – Specimens R33 under monotonic loading.

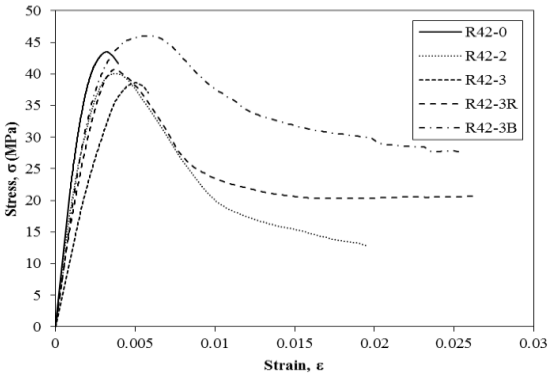

Figure 20. Stress-strain of concrete – Specimens R42 under monotonic loading.

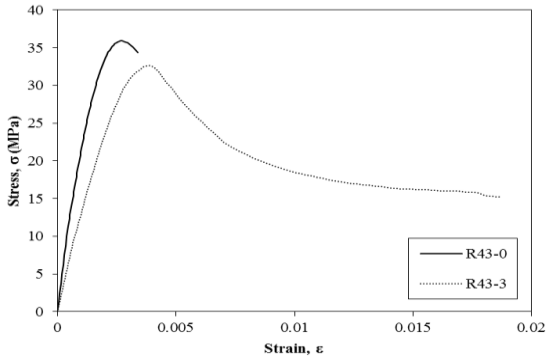

Figure 21. Stress-strain of concrete – Specimens R43 under monotonic loading.

Fig. 22 shows the effect of the amount of CFS used to confine the concrete samples, specimens C2 has an important contribution in terms of maximum stress, strain at maximum stress and maximum strain, while for square and rectangular shaped specimens, the maximum stress and strain at maximum stress remains at about the same values with a slight discrepancy. Specimens C2, S12, S13, R23, R32, R42 and R43 show an increment of the maximum strain according to the amount of CFS. The clear contribution of CFS on circular shaped specimens in terms of maximum stress, strain at maximum stress and maximum strain, occurs because the stress over the CFS tend to be uniform in case of circular shaped specimens unlike square and rectangular shaped specimens where the stress over the CFS is concentrated at the rounded corners.

Fig. 23 shows the effect of the radius R at the rounded corners of the square and rectangular shaped specimens tested, by comparing specimens with R=30mm and R=15mm, it can be observed that a larger radius helps to increase the maximum stress, the strain at maximum strain and the maximum strain. This occurs because the stress of CFS at the rounded corners of specimens of R=30mm has improved stress distribution in comparison with specimens of R=15mm.

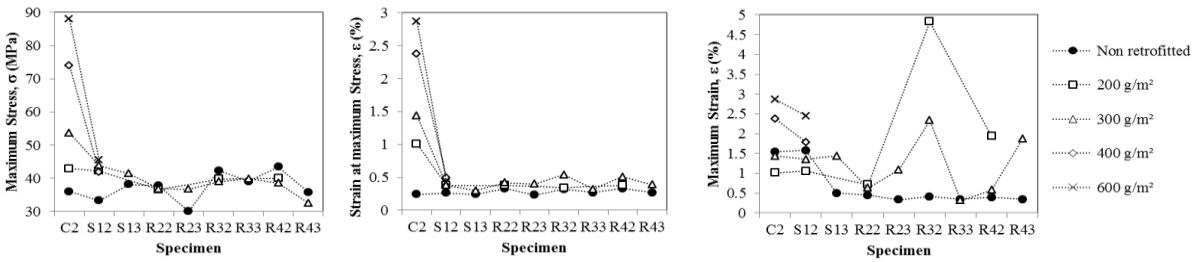

Figure 22. Effect of the amount of CFS

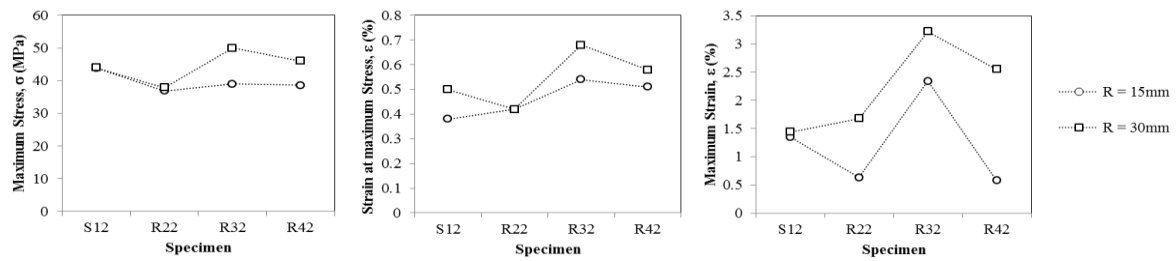

Figure 23. Effect of the chamfer radius

Fig. 24 shows the effect of the Young Modulus of CFS-2 (249000MPa) and CFS-3 (444000MPa) and its corresponding ultimate strain 1.88% and 0.73% respectively, where it displays an important contribution in terms of the maximum strain. This can be explained because CFS-2 has a larger ultimate strain than CFS-3. Therefore, CFS-3 has a brittle behaviour in comparison with CFS-2. For circular shaped specimen, the Young Modulus of CFS-2 shows an improved maximum strength and an improved strain at maximum stress, while for square shaped specimen remains about the same values.

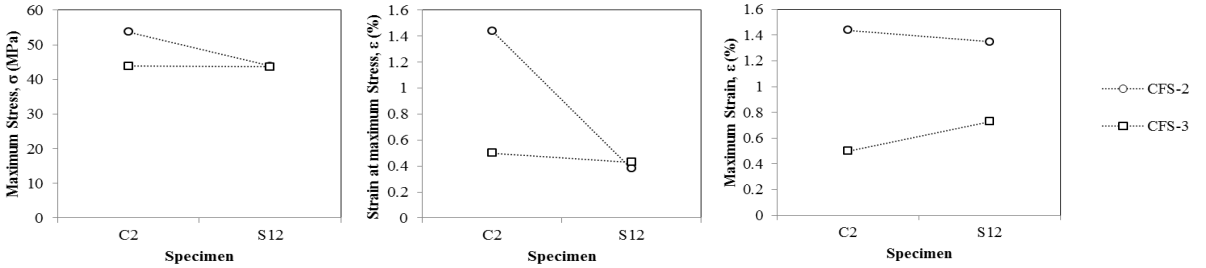

Figure 24. Effect of the young modulus of CFS

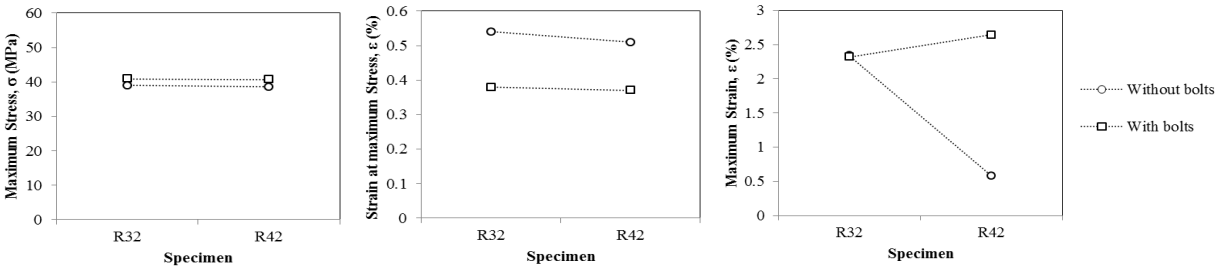

Figure 25. Effect of CFS fixed with bolts

Fig. 25 shows the effect of using bolts to fix the CFS to the rectangular specimens. It can be seen that the maximum stress remains about the same in both cases; the strain at maximum stress is improved without bolts, however the maximum strain is improved when bolts are used in specimen R42, this may happen because of the axial contribution of the steel plates attached to the specimens for fixing the bolts during the last stage of the test.

V. Conclusion

- Stress on the CFS in circular shaped specimens is distributed similarly on the CFS, while for square and rectangular shaped specimens the stress on the CFS is concentrated at corners.
- Carbon fiber sheet reinforcement increases the strain deformation capacity in all of the specimens.
- For rectangular shaped specimens, a larger chamfer radius helps to improve the maximum strain.
- Maximum strain of the specimens retrofitted with CFS is proportional to the ultimate strain of the CFS.
- Using bolts for fixing the CFS to the concrete sample does not have an important contribution in terms of maximum stress.

Acknowledgment

The main author wishes to thank the Japanese Government for the MEXT scholarship. Special thanks to Dr. Saito, the main author's supervisor, for his support and advice during his current doctoral studies. Last but not least, to Dr. Mastui and Dr. Hayashi for their valuable contribution to this research.

References

[1] C. Zavala, *et al*., "Cyclic behavior of low ductility walls considering perpendicular action," *Journal of Disaster Research*, vol. 8, no. 6, pp. 312-319, 2013.

[2] T. Matsui, T. Saito, and R. Reyna, "Basic study on reinforced concrete shear walls without boundary columns retrofitted by carbon fiber sheets," *Journal of Disaster Research*, vol. 9, no. 6, pp. 1008-1014, 2014.

[3] L. Lam and J. G. Teng, "Design-oriented stress–strain model for FRP-confined concrete," *Construction and Building Materials*, vol. 17, no. 6, pp. 471-489, 2003.

[4] L. Lam and J. G. Teng, "Design-oriented stress–strain model for FRP-confined concrete in rectangular columns," *Journal of Reinforced Plastics Composites*, vol. 22, no. 12, pp. 1149-1186, 2003.

[5] L. Lam and J. G. Teng., "Stress–Strain model for FRP-confined concrete under cyclic axial compression," *Engineering Structures*, vol. 31, no. 2, pp. 308-321, 2009.

[6] T. Nakatsuka, K. Kenichi, and T. Kinya, "Stress–strain characteristics of confined concrete with carbon fiber sheet," *Concrete Research and Technology*, vol. 9, no. 2, pp. 65-78, 1998.

Roy Reyna, (Peru, 1982). He received the B.Sc. degree in Civil Engineering from the National University of Engineering, Peru, in 2007, and the Master of Disaster Management Degree from the National Graduate Institute for Policy Studies, GRIPS-BRI-IISEE, Japan, in 2012. He joined the Architecture and Civil Engineering Department of Toyohashi University of Technology, Japan, as a Ph.D. Student, in 2013.

In 2009, he joined the Laboratory of Structures of the Japan-Peru Center for Earthquake Engineering and Disaster Mitigation (CISMID) as a research assistant and in 2012 became an associate researcher. His

research interests include base isolation system, non-linear hysteresis models; numerical simulation of buildings, his current research is analysis of reinforced concrete retrofitted with carbon fiber sheets using non-linear final element method.

Ph.D. candidate Reyna has the following selected publications:

R. Reyna and T. Saito, "Numerical simulation of base isolated buildings during the Great East Japan Earthquake and a proposal for a design procedure of base isolation system in Peru," *Bulletin of the International Institute of Seismology and Earthquake Engineering*, vol. 47, pp. 103-108. Tsukuba, Japan, 2012.

L. Cardenas, R. Reyna, L. Estacio, and C. Zavala, "Implementation of database of masonry walls test: Review of existing test data in Peru," *Journal of Disaster Research*, vol. 9, no. 6, pp. 1008-1014, 2014